Pure Appl. Chem., Vol. 81, No. 12, pp. 2203–2224, 2009.
doi:10.1351/PAC-CON-09-07-07

Large polycyclic aromatic hydrocarbons: Synthesis and discotic organization*

Xinliang Feng‡, Wojciech Pisula†, and Klaus Müllen**

Max Planck Institute for Polymer Research, Ackermannweg 10, 55128 Mainz, Germany

Abstract: Polycyclic aromatic hydrocarbons (PAHs) have attracted enormous interest due to their unique electronic and optoelectronic properties as well as the potential applications in organic electronics. This article reviews the progress in the modern synthesis of large PAHs with different sizes, shapes, edge structures, and substituents. Due to their outstanding self-organization characteristics, the discotic liquid-crystalline properties, self-assembled nanostructures on the surfaces, as well as the application in electronic devices will be discussed.

Keywords: discotic liquid crystals; hexabenzocoronene; nanographene; polycyclic aromatic hydrocarbons; self-assembly.

INTRODUCTION

Polycyclic aromatic hydrocarbons (PAHs) are a class of unique compounds that consist of fused conjugated aromatic rings and do not contain heteroatoms or carry substituents [1]. These compounds can be point source (e.g., oil spill) or non-point source (e.g., atmospheric deposition) and are one of the most widespread organic pollutants. Some of them are known or suspected carcinogens, and are linked to other health problems. They are primarily formed by incomplete combustion of carbon-containing fuels such as wood, coal, diesel, fat, tobacco, or incense [2,3]. Tar also contains PAHs. Different types of combustion yield different distributions of individual PAHs which can also give rise to isomers. Hence, those produced from coal combustion are in contrast to those yielded by motor-fuel combustion, which differ from those produced by forest fires. Some PAHs occur within crude oil, arising from chemical conversion of natural product molecules, such as steroids, to aromatic hydrocarbons. They are also found in the interstellar medium, in comets, and in meteorites, and are a candidate molecule to act as a basis for the earliest forms of life [4].

As defined by the International Union of Pure and Applied Chemistry (IUPAC), the simplest PAHs are phenanthrene and anthracene. PAHs may contain four-, five-, six-, or seven-membered rings, but those with five or six are most common. PAHs comprised only of six-membered rings are called alternant PAHs. Certain alternant PAHs are called "benzenoid" PAHs. PAHs containing up to six fused aromatic rings are often known as "small" PAHs, and those containing more than six aromatic rings are called "large" PAHs. Due to the availability of samples of various small PAHs, the main research

Pure Appl. Chem.* **81, 2157–2251 (2009). A collection of invited, peer-reviewed articles by the winners of the 2009 IUPAC Prize for Young Chemists.
‡Corresponding author: E-mail: feng@mpip-mainz.mpg.de
†E-mail: muellen@mpip-mainz.mpg.de
**Current address: Evonik Degussa GmbH, Process Technology & Engineering, Process Technology - New Processes, Rodenbacher Chaussee 4, 63457 Hanau-Wolfgang, Germany

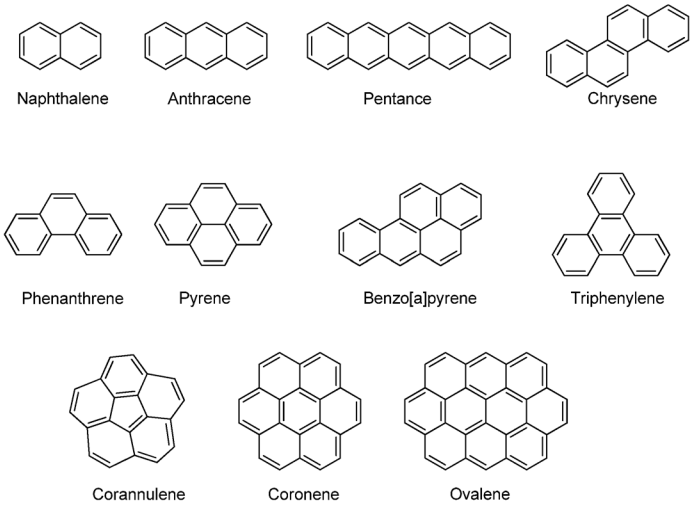

Fig. 1 Examples of prominent PAHs.

on PAHs has been focused on those of up to six rings. Examples of well-known PAHs are shown in Fig. 1.

In graphene, the PAH motif is extended to large 2D sheets, which can be regarded as graphene or graphite segments (Fig. 2), and represents one of the most intensively investigated class of compounds in synthetic chemistry and materials science. The systematic study of PAHs and their application as materials have spurred scientist for several decades, however, only a few selective synthetic methods have been established so far. Fundamental contributions to the directed synthesis and characterization of polycyclic aromatics were pioneered by R. Scholl, E. Clar, and M. Zander, who achieved the synthesis of numerous aromatic compounds under drastic conditions at high temperatures with strong oxidation [5–10]. The synthetic breakthrough was achieved as a result of progress of analytical techniques and made the selective synthesis of various PAHs under mild conditions possible [11].

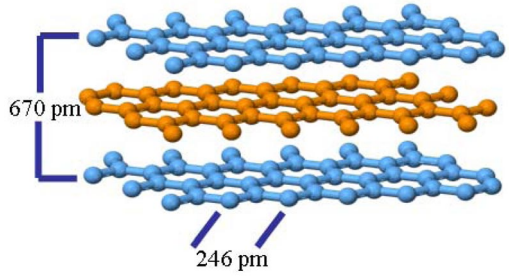

Fig. 2 Layer structure of graphite.

One of the intrinsic properties of the PAHs is their aromaticity, which has attracted great interest in theoretic chemistry [12], different theoretical methods have been applied to estimate the electronic properties of graphite based on PAHs with increasing size and varying topologies. As a result of the development of organic semiconductors [13], PAHs with unique electronic and optoelectronic properties have received great attention in the scientific community. Large PAHs terminated by hydrogen, alkyl substituents, and functional groups, which endow a facile solution processing, are promising candidates in organic devices such as light-emitting diodes (LEDs), field-effect transistors (FETs), and photo-

volatic cells [14,15]. Additionally, 2D all-benzenoid graphitic molecules with appropriate substituents are fascinating due to their highly stable columnar mesophases, which are desirable for device processing [14–16]. Furthermore, well-defined nanostructures resulting from supramolecular self-assembly of PAHs, such as nanotubes and nanowires, have a great potential in nanotechnology [17–19].

SYNTHESIS

Besides small PAHs, which have been isolated from coal tar and catalytic hydrocarcking of petroleum, a far more defined preparation of PAHs is possible by means of synthetic organic chemistry, as shown by the pioneering work of R. Scholl, E. Clar, and M. Zander. The most generally used methods for the construction of PAH ring systems are summarized in the following section, including the most recently developed synthetic methodologies, and indicate the trend of this research field toward the development of milder methods, which proceed with high regioselectivity and yields.

Intra- and intermolecular Diels–Alder reaction

Diels–Alder reaction is surely one of the most efficient synthetic methods to create carbon–carbon bonds. One of the recent examples is to synthesize the pentacene derivative as illustrated in Fig. 3. Maleic anhydride and quinones, such as benzoquinone, are frequently employed as dienophiles for this purpose. Here the double Diels–Alder strategy of Danieshefsky's diene with anthradiquinone affords a cycloadduct that is finally converted to the substituted pentacene **1** by reductive deoxygenation/aromatization [20].

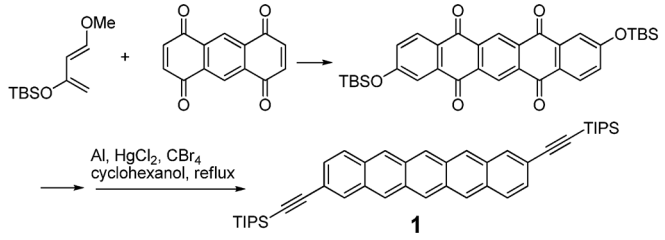

Fig. 3 Example of Diels–Alder cycloaddition for the synthesis of PAHs.

An elegant entry to oligophenylene structures can be achieved by intramolcular [4+2] cycloaddition of suitable phenylene-vinylene derivatives, followed by aromatization of the newly formed cyclohexene structures. An example for such strategy is a suitable precursor for a 60 carbon-containing, rhombus-shaped PAH **5** (Fig. 4) [21,22]. The para-terphenyl derivative **2** is subjected to a nearly quantitative intramolecular [4+2] cycloaddition at 135 °C to form the cyclohexene derivative **3**. Following the mild oxidation with 2,3-dichloro-4,5-dicyanoquinone (DDQ) and $CuCl_2/AlCl_3$, the precursor is planarized to the desired molecule **5**.

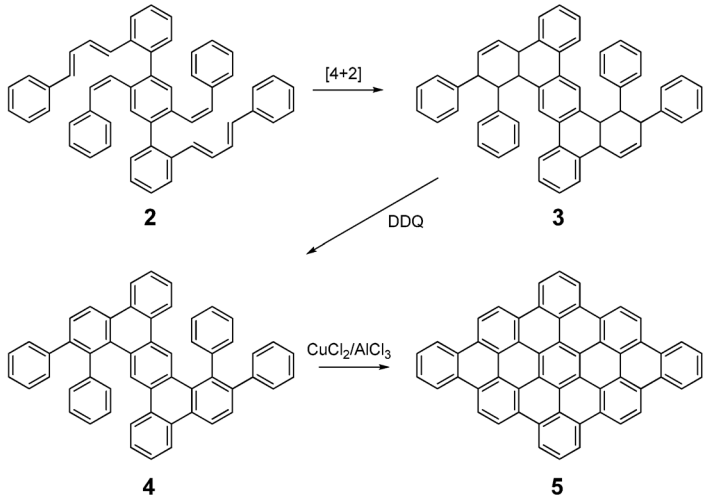

Fig. 4 Synthesis of rhombus-shaped PAH **5**.

Ring-closing olefin metathesis (RCM)

Strategies involving transition-metal catalysis are attractive because of the mild reaction conditions. For example, palladium-catalyzed cross-coupling is popular for the formation of aryl-aryl σ-bonds. RCM has emerged as a powerful tool for the preparation of double bonds in cyclic organic compounds but has only recently been applied to PAHs. The first preparative utility of RCM to generate functionalized phenanthrenes is from 2,2'-divinylbiphenyl derivatives. As a typical example shown in Fig. 5, the double RCM of terphenyl precursors affords dibenz[*a*,*j*]anthracene **6** and dibenz[*a*,*h*]-anthracene **7** in good yields [23,24].

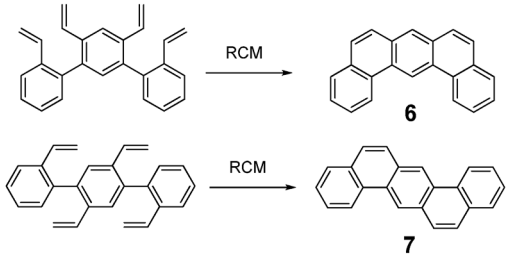

Fig. 5 Double RCM synthesis of acenes.

The need for more highly substituted and structurally varied helicenes has led to the development of new methods as replacements of the classical synthesis by the photocyclization of stilbenes. As a result, very recently, RCM has also been used to synthesize the substituted [5]helicenes **8** and even [6]- and [7]helicenes in good to high yields (Fig. 6) [25].

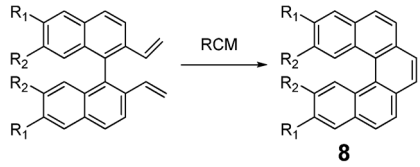

Fig. 6 Preparation of substituted helicenes.

Benzannulation and electrophilic cyclization

The published methods for the synthesis of coronenes **9** are plagued with long procedures and inefficiency, typically including a pyrolysis step at high temperatures. The lack of a convenient and efficient synthesis of coronenes impedes their progress in organic chemistry. Scott and co-workers firstly proposed a short synthesis of coronenes from metal-catalyzed benzannulation of bis(1,1-ethynyl)alkene species [26], which was a useful precursor for the flash-vacuum pyrolysis (FVP) synthesis of coronenes and could be prepared conveniently in three steps from commercially available anthraquinone (Fig. 7). By using 20 mol % $RuPPh_3(cymene)Cl_2$ catalyst, a 15~20 % yield of coronene was for the first time obtained by chemical reactions in solution, which is already much higher than that of the FVP method. Liu and co-workers optimized the reaction conditions by using $TpRuPPh_3(CH_3CN)_2PF_6$ as catalyst, amazingly, an 86 % yield of coronene could be achieved [27]. By using their conditions, coronene derivatives with various substituents could be synthesized for the first time. This synthetic strategy can also be utilized for the synthesis of oligoacene derivatives, such as compound **7**.

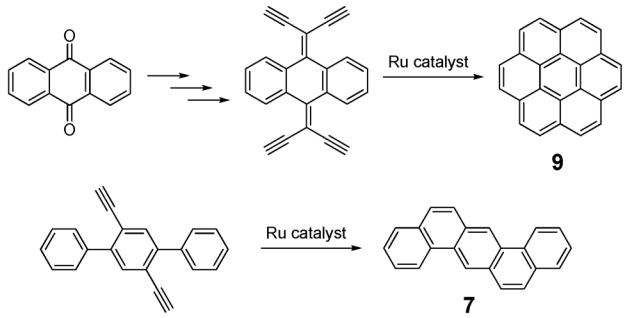

Fig. 7 Examples for the synthesis of PAHs by benzannulation.

With the goal of ultimately preparing polymeric fused or ribbon-like PAHs, Swager and co-workers have successfully developed the electrophilic cyclization to build up polyacences by using the strong electrophilic iodine reagent $I(pyridine)_2BF_4$ or trifluoroacetic acid [28,29]. The reaction conditions were very mild and mostly provided high yields. The typical example is shown in Fig. 8, starting from the conjugated polymers with 2,5-substituted diphenylacetylene units, conjugated ladder polymers or graphite ribbon **10** could be constructed in quantitative yields. The same synthetic protocol is also useful for the building of related oligoacenes and thioacenes. Larock and co-workers observed that ICl was a strong electrophilic reagent for this reaction, and could be widely used under mild conditions with high yields [30].

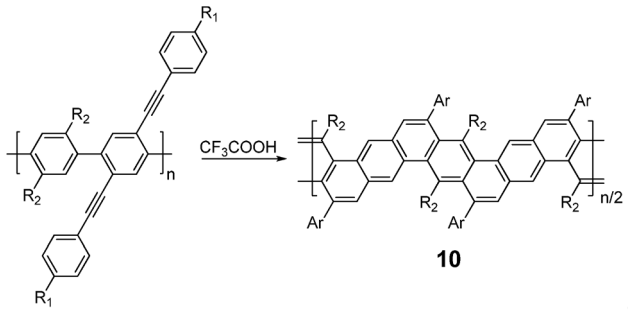

Fig. 8 Synthesis of polyacene by electrophilic cyclization.

Intramolecular photocyclization of stilbene-type compounds

The photoinduced ring closure of stilbene-type compounds has been extensively used in the preparation of condensed PAHs [31–33]. Different stilbenes can be conveniently prepared by employing Wittig–Heck as well as McMurry coupling reactions. Therefore, various PAHs can be easily made, for example, circumanthracene **11** (Fig. 9).

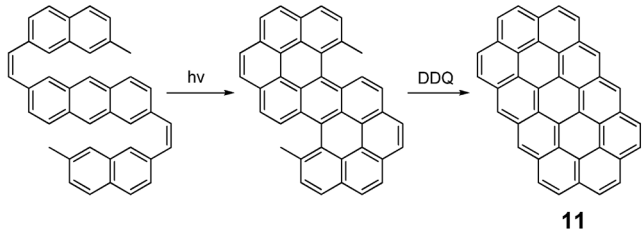

Fig. 9 Synthesis of circumanthracene.

Very recently, Nuckolls and co-workers have developed a novel approach toward a phase-forming, distorted hexa-*cata*-hexabenzocoronene derivative **12** (Fig. 10) [34], whereby the decisive step is accomplished by the photocyclization. The material formed columnar liquid-crystalline phases with high charge-carrier mobilities as determined in FETs.

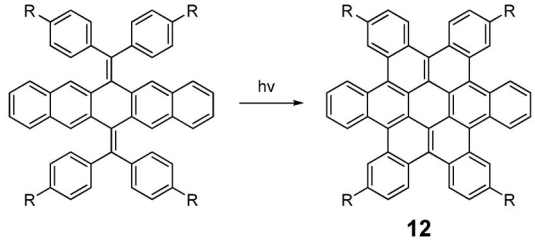

Fig. 10 Synthesis of hexa-*cata*-hexabenzocoronenes.

Flash-vacuum pyrolysis

The conversion of appropriate precursors to condensed PAHs at high temperature with short contact time in the hot zone is referred to as flash-vacuum pyrolysis (FVP). The key point is the design of the

precursors, which should have a good thermal stability and reactive sites. A typical example is the synthesis of corannulene **13** in good yield (Fig. 11) upon the treatment of 7,10-bis(1-chlorovinyl)fluoranthene under FVP condition [35,36]. This synthetic method has been successfully developed to yield different bowl-shaped PAHs and fullerenes [37–39].

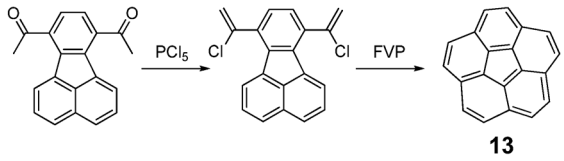

Fig. 11 Synthesis of corannulene by FVP method.

Oxidative cyclodehydrogenation

In the presence of Lewis acid catalysts, the intermolecular or intramolecular coupling of two aromatic rings is called the "Scholl reaction". The detail mechanism for this reaction is, however, still not yet clearly understood. A stepwise arenium cation mechanism and a radical cation mechanism are suggested theoretically [40,41]. With appropriate oligophenylene precursors, the Scholl reaction has been developed as a powerful tool to produce various all-benzenoid PAHs [14,15]. A typical example is the synthesis of hexa-*peri*-hexabenzocoronenes (HBCs) **15** and their derivatives (Fig. 12) from substituted hexaphenylbenzene precursors (**14**) by treatment with iron(III) chloride or $AlCl_3$-$Cu(OTf)_2$.

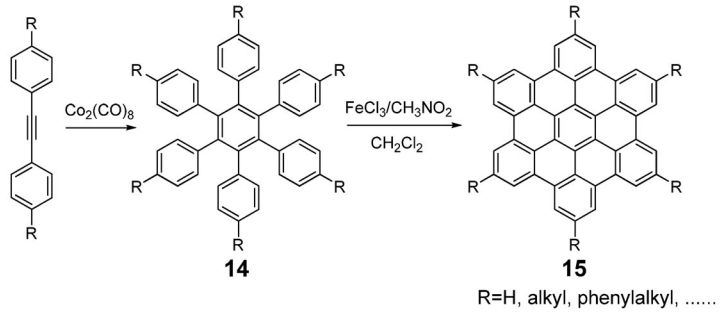

Fig. 12 General synthesis of D_6 symmetric HBCs.

A simple approach to HBCs with D_6 symmetry is starting from the $Co_2(CO)_8$ catalyzed cyclotrimerization of diphenylacetylenes to afford hexaphenylbenzene derivatives (Fig. 12). It opens up the possibility to introduce solubilizing alkyl side-chains as well as functional groups on HBCs, and renders them into ordered columnar liquid-crystalline phases. An extraordinary versatile route to prepare differently symmetric hexaphenylbenzenes is the Diels–Alder reaction of tetraphenylcyclopentadienones (CPs) with diphenylacetylenes (Fig. 13). The versatility of this concept becomes obvious regarding the defined preparation of HBC derivatives of different substitution types. By variation of the substituents in the diphenylacetylene or CP, it is possible to furnish different substitution patterns as shown in Fig. 13, such as mono-substituted, "ortho"-disubstituted (C_2 symmetry), and "para"-disubstituted (D_2 symmetry) HBCs.

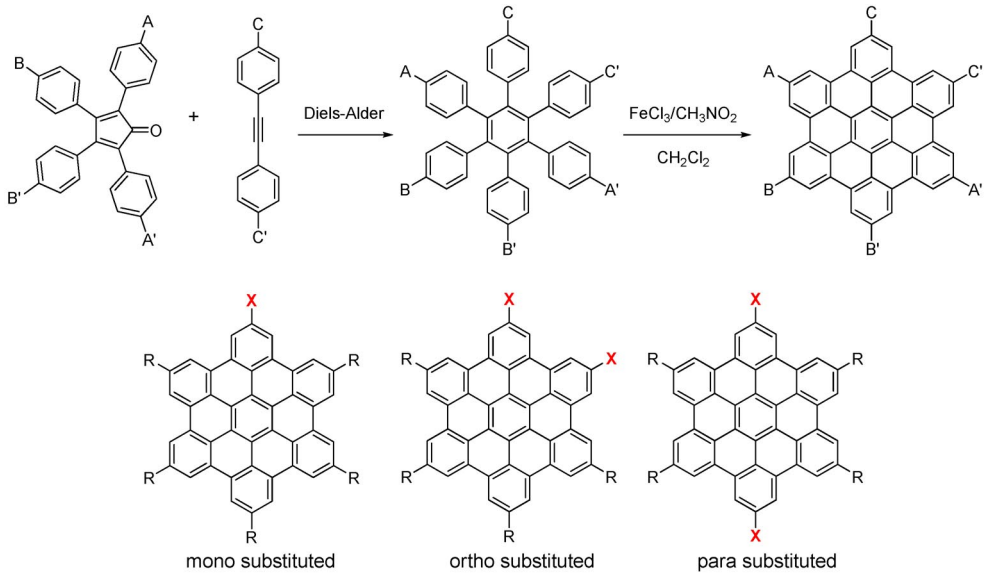

Fig. 13 General synthesis of low symmetric HBCs. Different substitution patterns of HBC derivatives (X indicates alkyl substituents or functional groups).

Very recently, a series of "para" symmetrically and unsymmetrically substituted hexaphenylbenzene analogs could be accomplished by using a sterically hindered Suzuki coupling reaction of arylboronic acid with 1,4-diiodo-2,3,5,6-tetraarylbenzenes under optimized reaction conditions [42]. This synthetic strategy offers remarkable opportunities to achieve various "para"-disubstituted (D_2 symmetry) and unsymmetric HBCs (Fig. 14). In particular, the synthesis of push–pull structure (donor–HBC–acceptor) based on the HBC can be realized for the first time [43].

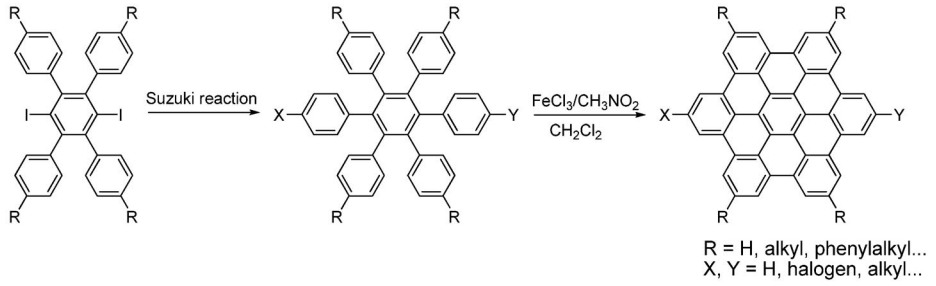

Fig. 14 Synthesis of HBCs based on the Suzuki coupling approach.

Although the synthesis of HBCs with D_6 symmetry and low symmetry have been widely made, the obstacles to access HBCs with C_3 symmetry was only resolved quite recently [44–49]. While the cyclotrimerization of symmetric diphenylacetylenes allows the synthesis of D_6 symmetric hexaphenylbenzenes and thus D_6 symmetric HBCs, two isomers are formed when asymmetric diphenylacetylenes are used and are normally difficult to be separated [47–49]. By optimizing the different polarity between two substituents on the asymmetric diphenylacetylenes, after cyclotrimerization, the isomers can be separated by columnar chromatography (Fig. 15). On the basis of this synthetic concept, a class of C_3 symmetric HBCs with alternating polar/apolar substituents can be obtained [47–49]. These HBCs car-

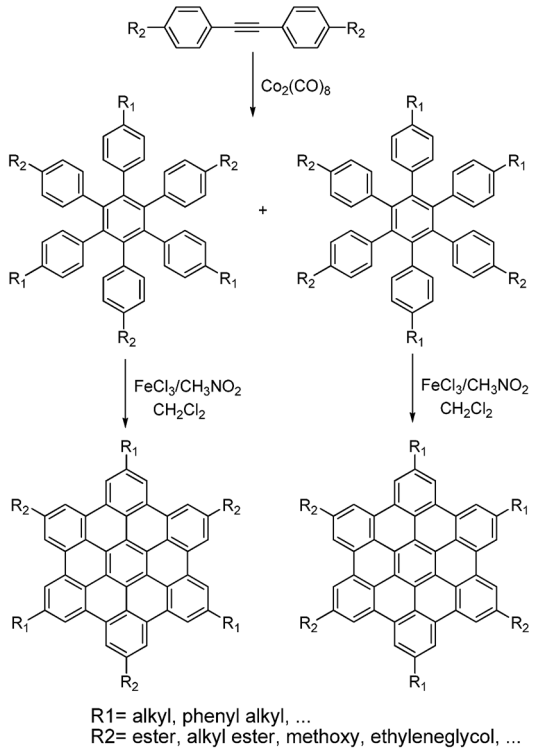

Fig. 15 Synthetic route toward C_3 symmetric HBCs with alternating polar/apolar substituents.

rying three solubilizing alkyl chains and three functional groups, such as ester groups and methoxy groups, thus enable a high level of control over the self-assembly in solution, in bulk and on the surface. Furthermore, asymmetric HBCs can also be derived by this synthetic route.

By contrast to the conventional route with using hexaphenylbenzene as precursors, a novel design of suitable 1,3,5-tris-2'-biphenylbenzene derivatives also enables a versatile synthesis of a class of C_3 symmetric HBCs (Fig. 16) [44,46]. Hence, a key building block 1,3,5-tris-2'-bromophenylbenzene **16** was synthesized firstly in an efficient way, and allowed single or multi-step transition-metal-catalyzed coupling reactions to provide a series of C_3 symmetric 1,3,5-tris-2'-biphenylbenzene precursors. After the final treatment with $FeCl_3$ under mild conditions, D_3 symmetric HBC with three alkyl substituents (**17**) and C_2 symmetric HBC with two alkyl substituents (**18**) were both obtained from this route [46]. In addition, the building block **15** can be further extended to synthesize a series of C_3 symmetric dendritic 1,3,5-tris-9'-phenanthrenylbenzene and other substituted 1,3,5-tris-2'-arylbenzene precursors, thus providing the possibility to access a class of triangle-shaped (**19**, **20**) and semi-triangle-shaped PAHs (**21**) [45].

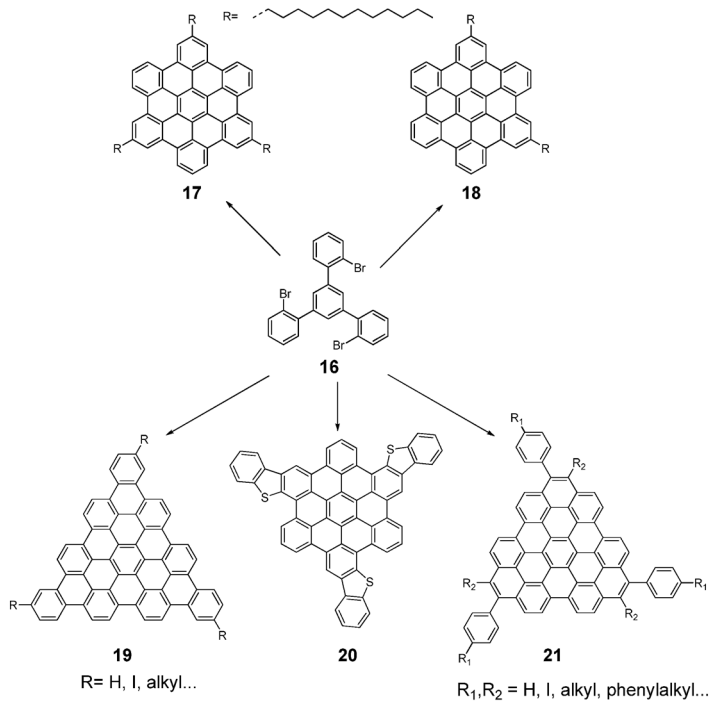

Fig. 16 The versatile synthesis of C_3 symmetric HBCs and triangle-shaped discotics based on the key building block **16**.

Obviously, one of the major goals of large PAH synthesis is to produce improved and structurally defined model compounds of graphene. By employing the previous concept, large dendritic oligophenylene precursors with different size and shape were designed by using the Diels–Alder reaction or cyclotrimerization based on suitable building blocks. After planarization of these precursors, all kinds of large benzenoid PAHs with different molecular sizes, symmetries, and peripheries have been available (Fig. 17). Up to now, the largest PAH (**24**) with disc shape containing up to 222 carbon atoms is accessible [50]. Other large PAHs with, e.g., cordate-shape (C96, **22**), square-shape (C114, **23**), and others are also attainable [51,52].

Based on the established sterically hindered Suzuki reaction conditions (Fig. 18), low polydispersed hexaphenylbenzene-type polymers can be constructed, which can then be cyclodehydrogenated to obtain 1D graphene nanoribbons **25** [53]. These soluble nanoribbons with lengths of up to 12 nm can be fully characterized by UV/vis absorption spectroscopy, mass spectrometry, as well as scanning tunnelling microscopy (STM), which by all means support the successful cyclodehydrogenation of large polyphenylene systems. Therefore, this organic chemistry approach presents an intelligent concept toward the synthesis of structurally perfect graphene nanoribbons, which can never be accessed by physical exfoliation and lithography methods.

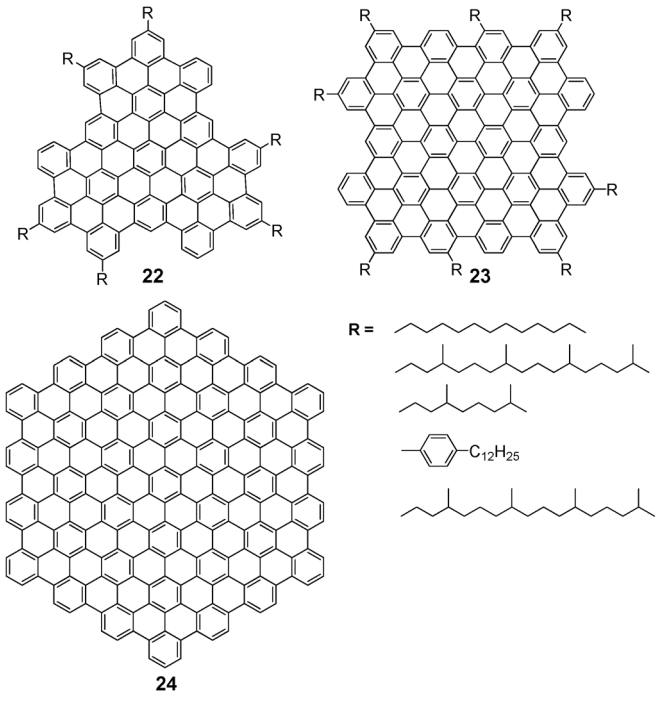

Fig. 17 Chemical structures of several large PAHs.

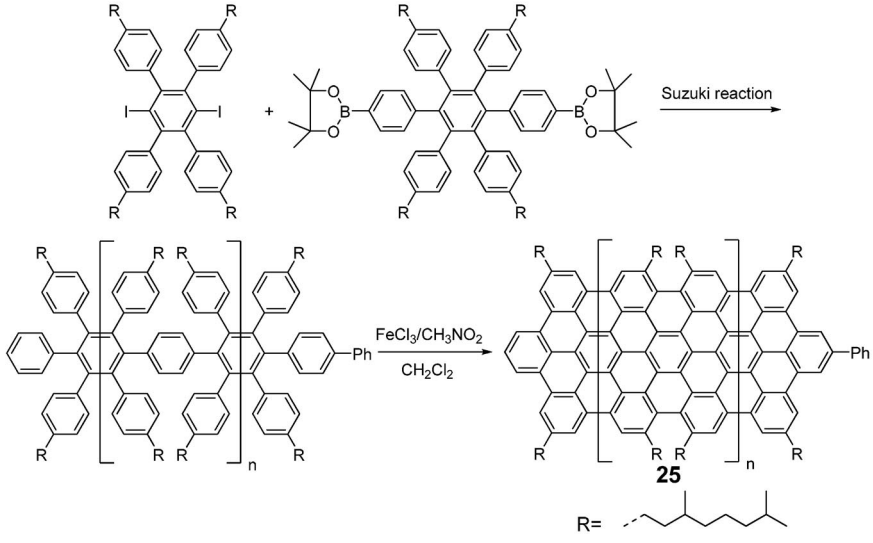

Fig. 18 Synthesis of graphene nanoribbons.

The most recent progress in the synthesis of large PAHs is the inclusion of additional double bonds on the periphery of HBCs, which act as the "zigzag" armchair. It is well known that the armchair with double bond-like characteristics will dramatically influence the electronic and optoelectronic properties of PAHs, as well as their chemical reactivities [54,55]. Up to now, HBCs with mono-, double-, and tri-zigzag have been successfully synthesized (Fig. 19) [45,56,57]. In addition to the achievement

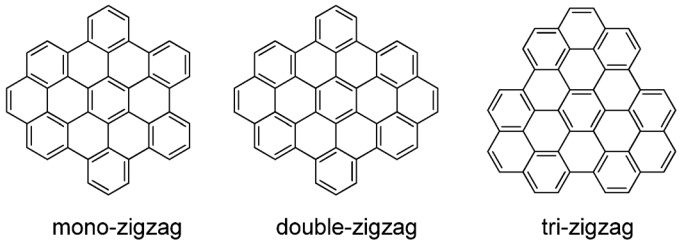

Fig. 19 HBCs with different zigzag peripheries.

of all-hydrocarbon-based nanographene building blocks, electron-rich and -poor heteroatoms such as sulfur and nitrogen have also been successfully incorporated into the nanographene units [48,58]. The further functionalization and modification based on these building blocks will be the future focus.

SELF-ORGANIZATION AND DISCOTIC LIQUID CRYSTALS (DLCs)

Introduction and materials

The hierarchical self-assembly of disc-shaped molecules leads to the formation of DLCs [15,16,59,60]. Vorlander in 1908 established his rule that liquid-crystalline compounds must have a molecular shape as linear as possible. All the liquid-crystalline materials prepared over about 90 years belonged to this family. However, in 1977 S. Chandrasekhar reported that not only rod-like molecules, but also compounds with disc-like molecular shape are able to form mesophases [61]. It was established that a number of benzene-hexa-*n*-alkanonates, from thermodynamic, optical, and X-ray studies, can form a new class of LCs in which molecules are stacked one on top of the other within columns that further assemble in a hexagonal arrangement. DLCs essentially consist of three types of mesophases, with varying degrees of organization: columnar (col), nematic-discotic (N_d), and lamellar discotic, where the structure of the latter has not yet been fully elucidated (Fig. 20) [62]. Three 2D lattices are possible in a mesophase of columnar structure: hexagonal, rectangle, or oblique as shown in Fig. 21. The discs are either perpendicular or slightly tilted with respect to the columnar axis.

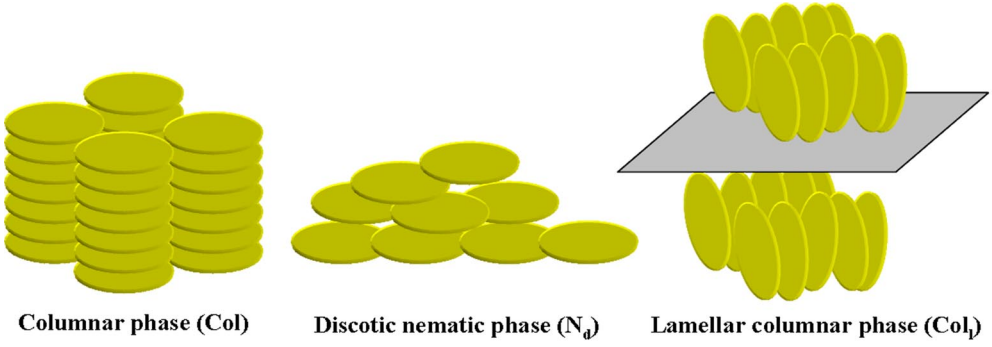

Fig. 20 Schematic representation of different mesophases of DLCs.

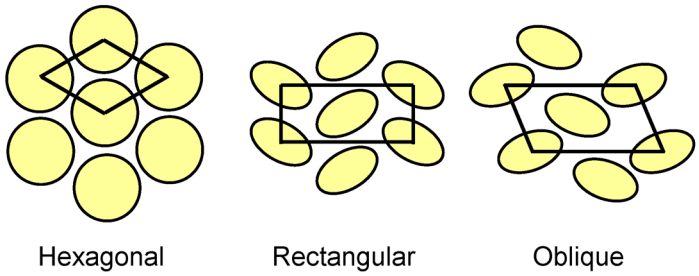

Fig. 21 Top view of 2D lattices of columnar phases. The ellipses denote discs that are tilted with respect to the columnar axis.

A majority of DLCs form columnar mesophases probably due to the phase separation between the rigid aromatic core and peripheral flexible side-chains as well as intense π–π interactions of aromatic cores. The core–core separation in a columnar mesophase is usually of the order of 3.5 Å so that there is considerable overlap of π-orbitals. As flexible long aliphatic chains surround the core, the intercolumnar distance is usually 20–40 Å, depending on the lateral chain length. Therefore, the interactions between neighboring molecules within the same column would be much stronger than interactions between neighboring columns. Consequently, charge migration in these materials is expected to be quasi-1D and anisotropic. Conductivity along the columns in the columnar mesophases has been reported to be several orders of magnitude higher than in the perpendicular direction [63–65]. Thus, the columns may be described as molecular wires (Fig. 22). So far, charge-carrier mobility as high as 1.1 $cm^2\ V^{-1}\ s^{-1}$ along the columns has been observed for HBC at the crystalline phase [66].

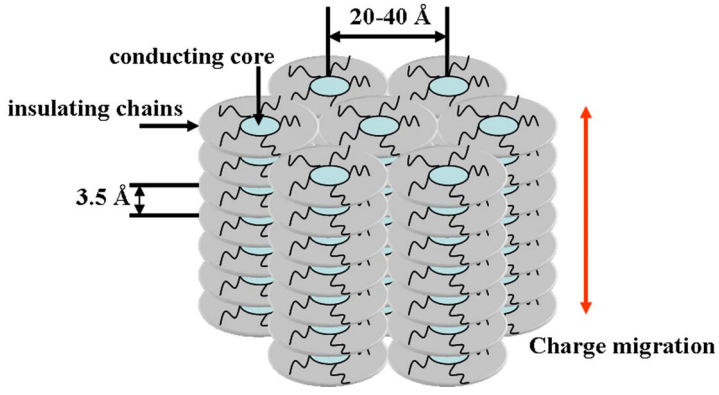

Fig. 22 Schematic view of charge migration in columnar phase.

The supramolecular assemblies of disc-shaped molecules have been extensively studied for the energy and charge migration in organized systems and their device applications, such as 1D conductors, photoconductors, LEDs, photovoltaic solar cells, FETs, and gas sensors have been sought [67,68]. Currently, the number of DLCs derived from more than 50 different cores comes to about 3000. In Fig. 23, some of the most prominent DLCs are shown, which range from the first reported hexa-alkanoyloxy-benzenes to porphyrins, phthalocyanines, triphenylenes, hexaazatriphenylenes, perylenes, macrocycles, HBCs, and others [69–78].

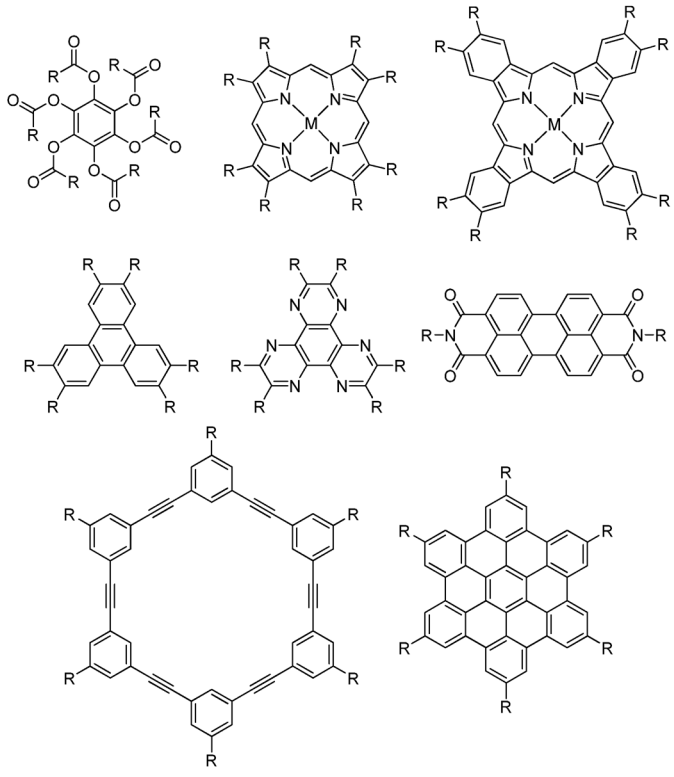

Fig. 23 Selection of prominent DLCs.

Characterization of the self-organization

In order to gain deep understanding of the molecular ordering in the bulk phase of discotics, thermogravimetric analysis (TGA), differential scanning calorimetry (DSC), polarized optical microscopy (POM), and X-ray diffractometry are necessary tools for structural characterizations. DSC, POM, and X-ray reveal the columnar packing in different phases. Solid-state NMR spectroscopy is an additional valuable tool to probe the packing mode at the molecular scale. Sometimes, solid-state UV–vis spectroscopy, atomic force microscopy (AFM), scanning electron microscopy (SEM), and transmission electron microscopy (TEM) can also be combined to understand the phase transitions, and self-organization in thin layers upon the thermal annealing in the mesophase.

For the alkyl substituted HBCs, TGA revealed that the derivatives are stable up to 400 °C, at which temperature decomposition of the substituted alkyl chains starts [15]. Three phases are typically observed (Fig. 24); both X-ray and solid-state NMR experiments revealed a tilted columnar organization in the crystalline phase, in which the aromatic core is crystallized and positioned on fixed lattice points. In the mesophase, the rotation of HBC discs around the column axis is possible, and the discs are perpendicular to the columnar axis. In the isotropic phase, the materials behave like the normal liquid without anisotropy. Two-dimensional wide-angle X-ray scattering measurements of extruded fibers are surely one of the most important methods to extract detail information about supramolecular organization of HBCs in the solid state (Fig. 25) [79]. The 2D patterns with information regarding the stacking within the columns and the intercolumnar arrangement in different phases are then obtained.

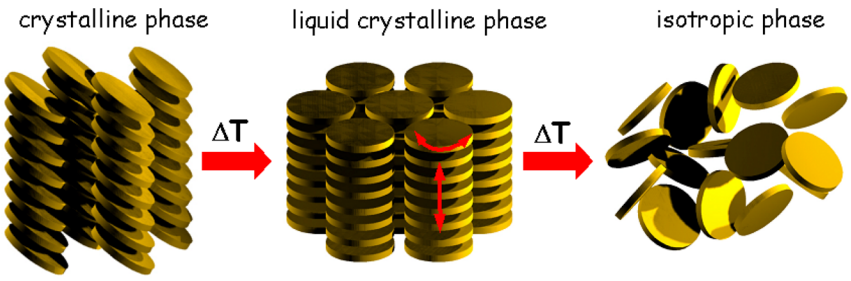

Fig. 24 Schematic representation of the self-organization within three phases of substituted HBCs.

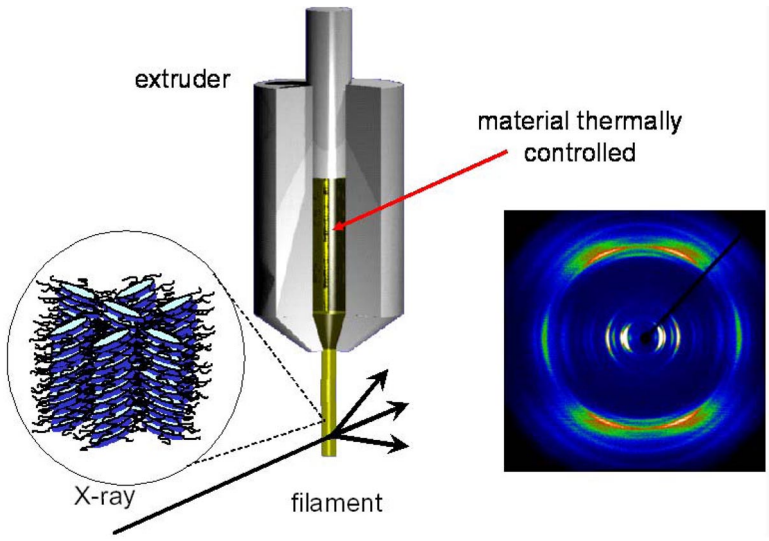

Fig. 25 Schematic illustration of the experimental set-up and principle for 2D WAXS measurements on extruded filaments.

Self-assembly of discotics on the surface

In the quest for the fabrication of miniaturized devices based on molecular objects and nanostructures, the self-assembly of conjugated π-molecules on the surfaces are essentially important. There are basically two approaches to this research field, the first one is grounded on the visualization and manipulation of single molecules or small aggregates, which is named as single molecular electronics; the second field is based on the fabrication of nanostructures in the device, such as nanofibers (nanowires), nanotubes, and nanospheres, which has been spurred intensively in the recent years.

STM makes it possible for the first time to generate real-space images of PAHs with a resolution at the submicrometer scale. The ultra-high vacuum deposition (UHV) STM is limited to small molecules which are easy to be sublimed. Therefore, only a few HBC derivatives could be deposited due to the relative high sublimation temperature. Using soluble, alkyl substituted HBC derivatives, face-on monomolecular layers could be prepared by self-assembly from solution on highly oriented pyrolytic graphite (HOPG), and could be analyzed with STM at the liquid–solid interface [80]. This methodology represents a useful approach to study the self-assembly behavior of molecules on the surface, which can be solution-processable. Figure 26 shows the ordering pattern of hexadodecyl-HBC (HBC-C12) on HOPG. Due to their specific areas of the molecules, the study by scanning tunnelling spectroscopy (STS) revealed different current–voltage curves for the aromatic and the aliphatic areas [81]. Very re-

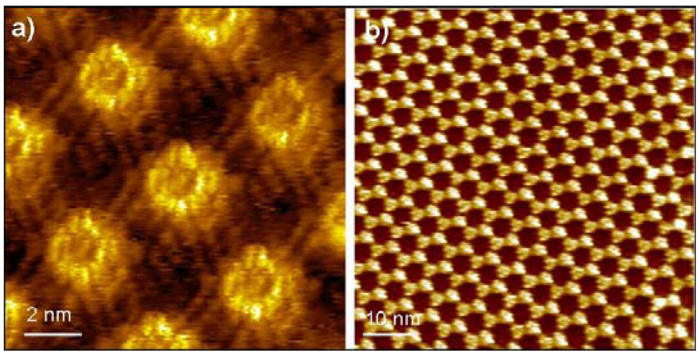

Fig. 26 Self-assembly of HBC-C12 (a, compiled from ref. [80]) and triangle-shaped PAH **21** (b, compiled from ref. [82]) on the liquid–solid interface.

cently, C_3 symmetrical triangle-shaped discotics are observed to self-assemble into ordered honeycomb networks [45], the driving force could be ascribed to the molecular interface and molecular–molecular interactions, therefore allowing potential applications in molecular switches and host–guest recognitions [82]. On the other hand, at the n-tetradecane/graphite interface, HBC-C12 can spontaneously form uniaxial columnar stacks on graphite. These nanocolumns are aligned horizontally on the substrate, with individual molecules in edge-on orientation, and are adsorbed on an intermediate face-on HBC-C12 monolayer into [HOPG/face-on/edge-on] self-organized systems [83].

In general, columnar nanostructure growth through strong π-stacking of alkylated discotic building blocks combined with additional intermolecular forces are attractive, both as "nanowires" and as molecular systems forming uniform films with a high degree of columnar orientation [84,85]. Recently, HBCs self-assembled into well-defined nanotubular or fibrous objects with a large number of π-stacked HBC units, have gained wide attention due to their semiconducting character [17–19].

In Fig. 27a, the optical microscopy depicts a pronounced aggregation propensity of an HBC-C12 after solution casting. The resulting drop-cast film consists of fiber-like structures when deposited on an FET. Each microfiber consists of the typical columnar stacks that form due to the π-stacking interactions of the HBC-C_{12} molecules. Charge-carrier transport takes place along the axis of the columns, the transistor shows a saturated hole mobility of $\mu_{sat} = 3 \times 10^{-4}$ cm^2/Vs and a source drain current on/off ratio of $I_{on}/I_{off} = 2 \times 10^5$. This moderate charge-carrier mobility can be related to macroscopic columns connecting the source and drain electrodes [86].

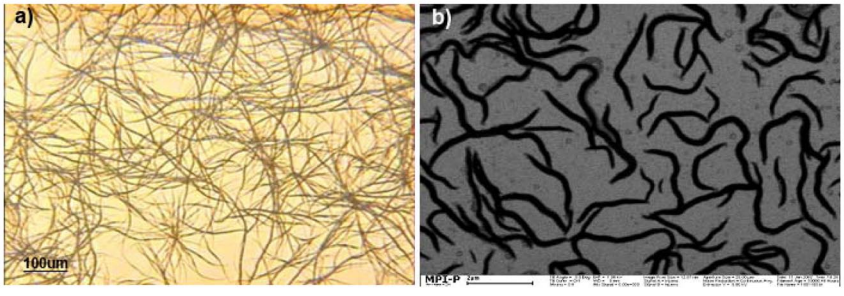

Fig. 27 Self-assembly of HBCs into fibrous nanostructure on the surface. (a) optical image of the morphology of HBC-C12 drop-cast from toluene (1.0×10^{-4} M) without cross-polarizers; (b) SEM image of C_3 symmetric HBC with alternating hydrophilic/hydrophobic substituents from MeOH:$CHCl_3$ = 2:1 solution (1.0×10^{-4} M), compiled from ref. [49].

Since the above-described method for fiber growth is strongly dependent on the nature of molecules, an appropriate way to fabricate fibers on the surface is to design new HBC molecules which can combine the strong π-stacking associated with additional noncovalent interactions [47–49]. C_3 symmetric HBCs with alternating hydrophilic/hydrophobic substituents allow control over the self-assembly in solution, in bulk, and on the surfaces, and thus are good candidates for this application. Figure 27b shows the fiber formation of this kind of HBC on the surface by facile casting from appropriate MeOH/$CHCl_3$ cosolvents [49].

DLCs for electronic devices

DLCs, which are formed by large PAHs, are attractive as charge-carrier transporting materials due to the formation of quasi-1D columnar structure. The hexahexylthioether substituted triphenylenes were the first examples of DLCs with high 1D charge-carrier mobility, whereby the highly ordered helical packing of discotics was expected to be the reason [87]. The formation of helical stacks does not only enhance the charge-carrier transport, but leads in addition to high stability of the supramolecular structures at elevated temperatures due to the improved interaction between molecules [45,47,57]. HBC and derivatives with larger rigid core compared with other mesogens allow large π-orbital overlap between the discs in the column. As a result, alkyl and alkylphenyl substituted HBCs possess a number of excellent properties such as high order, and the highest charge-carrier mobility (up to 1.13 $cm^2\ V^{-1}\ s^{-1}$) of all known DLC materials. The control of helical organization over HBC and extended PAH derivatives can be accomplished through the introduction of bulky phenyl groups [45,57,88]. The introduction of additional alternating hydrophilic/hydrophobic substituents even enables the staggered arrangement between every two molecules within the columnar superstructures [89]. Theoretic simulation of ideal system with this unique molecular organization indicates the charge-carrier mobility up to 15.9 $cm^2\ V^{-1}\ s^{-1}$ can be available, which is so far the highest value for all discotics. Considerable scientific and technological efforts have been devoted to DLCs for applications as active components in FETs, photovoltaic cells, and LEDs.

Organic field-effect transistors (OFETs)

The widespread interest in OFETs is based on the large-area coverage, high charge-carrier mobility and facile fabrication [19,90,91]. The self-assembly properties of columnar DLCs, in combination with their ability to provide anisotropic charge-carrier transport along the channel, make them viable candidates for OFETs. A typical OFET device is shown in Fig. 27 (left). For a p-type semiconductor, conduction of charge between the source and the drain electrodes is governed by the gate voltage. When the gate is positive with respect to the source, the semiconductor is depleted of carriers. When the gate is biased negatively, carriers accumulate in the channel between source and drain. The drain current is then proportional to the charge mobility. Long-range and edge-on organized discotic materials are crucial for the device application. The orientation of the disc can be controlled by different methods, such as shearing on a poly(tetrafluoroethylene) (PTFE) surface or zone-casting on the substrate [90,91]. The FET devices based on both methods show mobilities for aligned HBCs approaching $10^{-2}\ cm^2\ V^{-1}\ s^{-1}$.

Bulk heterojunction photovolatic cells

The photovoltaic effect requires [92]: (1) absorption of solar radiation and the photogeneration of excitions (electrons and holes); (2) polarization of the bound electron-hole pairs at the hetero-interface between donor and acceptor species; (3) charge separation, and the transport of the free charge carriers for collection at the cathode and anode. The typical bulk heterojunction photovoltaic device is shown in Fig. 28 (right).

Discotic materials based on HBC as donor together with perylene dyes as acceptor component have been successfully implemented in photovoltaic devices [93]. High external quantum efficiencies of greater than 34 % at 490 nm and power efficiencies up to 2 % have been achieved. The high efficiencies result from an efficient photoinduced charge transfer between HBC layers and perylene layers

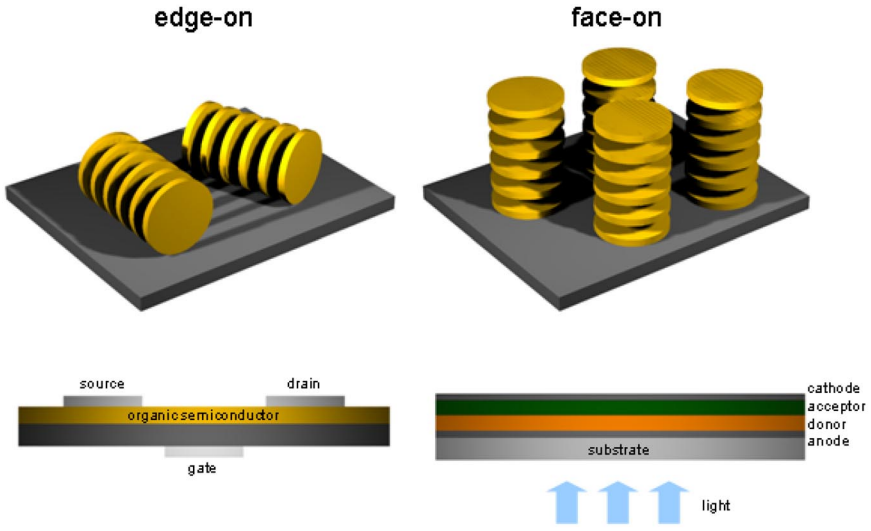

Fig. 28 Schematic representation of two different electronic device types and the desired arrangement of discotics as electronic materials.

and an effective charge transport through the layered structure. Triangle-shaped discotics consisting of extended graphene corona and swallow alkyl tails allow a facile purification, control over the thermotropic properties, and, finally, solution fabrication into efficient photovoltaic devices [94]. The unique design of large aromatic core provides a material with an extremely broad liquid-crystalline range, whereby the adequate choice of the substituent permits self-healing at low processing temperatures. It has been revealed that the latter aspect played a key role for the improved photovoltaic cells.

Organic light-emitting diodes (OLEDs)

Conjugated organic materials are capable of electroluminescence, and over recent years their potential applications in OLEDs have been of great interest. In a single-layer OLED, a thin film of an organic emitter is sandwiched between a transparent anode (ITO) and a metallic cathode. A multilayer device consists of separate hole-transporting layer, emitter layer, and electron-transporting layer. Electrons and holes, which are injected into the lowest unoccupied molecular orbital (LUMO) and highest occupied molecular orbital (HOMO), respectively, drift through the organic film under the influence of an applied electric field. The Coulumbic attraction between an electron and hole at the same chromophore site results in the formation of an exciton, a bound electron-hole pair, whose recombination produces luminescence. Efficient devices require the matching of energy levels to minimize the barriers for carrier injection and to trap both electron and holes exclusively in the emitter region. Initially, triphenylene-based DLCs were employed as hole transport materials [95]. More recently, OLEDs have been constructed using DLCs based on pyrene and perylene derivatives [96]. Some groups have explored the electroluminescence and charge-transport properties of photo-cross-linked and conjugated–bridged triphenylene derivatives in OLED applications [97].

CONCLUSION

PAHs have stimulated a great of interesting since the beginning of the 20th century. With the advances of research and application of conjugated oligomers and polymers in electronic devices, a lot of knowledge has been gained about the synthesis, structural characterization, and structure–property relationships of PAHs during the past 15 years. Modern synthetic organic chemistry developed in the past 30 years lays the foundation on the construction of large PAHs with different complexities. Efficient

routes have been established to prepare all-benzenoid and non-benzenoid PAHs with different sizes, shapes, edge-structures, and substituents. The major directions for future synthetic chemistry are the synthesis and characterization of extended PAHs, with different functional groups improving their processability, various chemical dopings tuning the electronic structure (e.g., B-N doped systems), periphery modification changing their chemical reactivity, and size expanding up to the physic limitation (50 nm) for graphene synthesis.

Large PAHs as a type of chemically stable semiconducting molecules are extremely interesting considering prolongation of the lifetime in electronic devices. Among them, the DLC materials based on these mesogens have many merits, including high charge-carrier mobility, easy solution processing, and self-healing properties, and thus are promising for practical device applications. Our targets in the future will be the design and synthesis of discotic materials with even higher charge-carrier mobility, which should take the consideration in terms of rational supramolecular design.

ACKNOWLEDGMENTS

Financial support by the Max Planck Society through the program ENERCHEM, the German Science Foundation (Korean-German IRTG) and DFG Priority Program SPP 1355 is gratefully acknowledged.

REFERENCES

1. J. C. Fetzer. *The Chemistry and Analysis of the Large Polycyclic Aromatic Hydrocarbons*, John Wiley, New York (2000).
2. K. F. Lang, J. Kalowy, H. Buffleb. *Chem. Ber. Recl.* **97**, 494 (1964).
3. K. F. Lang, J. Kalowy, H. Buffleb. *Chem. Ber. Recl.* **95**, 1052 (1962).
4. D. J. Cook, S. Schlemmer, N. Balucani, D. R. Wagner, B. Steiner, R. J. Saykally. *Nature* **380**, 227 (1996).
5. R. Scholl, C. Seer. *Justus Liebigs Ann. Chem.* **394**, 111 (1912).
6. R. Scholl, C. Seer. *Ber. Dtsch. Chem. Ges.* **44**, 1233 (1911).
7. E. Clar. *Ber. Dtsch. Chem. Ges.* **62**, 1574 (1929).
8. E. Clar. *Polycyclic Hydrocarbons*, Vols. 1 and 2, John Wiley, New York (1964).
9. E. Clar, M. Zander. *J. Chem. Soc.* 1577 (1958).
10. M. Zander. *Handbook of Polycyclic Aromatic Hydrocarbons*, Marcel Dekker, New York (1983).
11. S. Hagen, H. Hopf. *Top. Curr. Chem.* **196**, 44 (1998).
12. P. V. R. Schleyer. *Chem. Rev.* **101**, 1115 (2001).
13. T. A. Skotheim, R. L. Elsenbaumer, J. R. Reynolds (Eds.). *Handbook of Conducting Polymers*, 2nd ed., Marcel Dekker, New York (1998).
14. M. Watson, A. Fechtenkötter, K. Müllen. *Chem. Rev.* **101**, 1267 (2001).
15. J. Wu, W. Pisula, K. Müllen. *Chem. Rev.* **107**, 718 (2007).
16. S. Laschat, A. Baro, N. Steinke, F. Giesselmann, C. Hagele, G. Scalia, R. Judele, E. Kapatsina, S. Sauer, A. Schreivogel, M. Tosoni. *Angew. Chem., Int. Ed.* **46**, 4837 (2007).
17. J. P. Hill, W. Jin, A. Kosaka, T. Fukushima, H. Ichihara, T. Shimomura, K. Ito, T. Hashizume, N. Ishii, T. Aida. *Science* **304**, 1481 (2004).
18. Y. Yamamoto, T. Fukushima, Y. Suna, N. Ishii, A. Saeki, S. Seki, S. Tagawa, M. Taniguchi, T. Kawai, T. Aida. *Science* **314**, 1761 (2006).
19. S. Xiao, J. Tang, T. Beetz, X. Guo, N. Tremblay, T. Siegrist, Y. Zhu, M. Steigerwald, C. Nuckolls. *J. Am. Chem. Soc.* **128**, 10700 (2006).
20. C. P. Benard, Z. Geng, M. A. Heuft, K. VanCrey, A. G. Fallis. *J. Org. Chem.* **72**, 7229 (2007).
21. M. Müller, J. Petersen, R. Strohmaier, C. Günther, N. Karl, K. Müllen. *Angew. Chem., Int. Ed.* **35**, 886 (1996).
22. M. Müller, C. Kübel, K. Müllen. *Chem.—Eur. J.* **4**, 2099 (1998).

23. M. C. Bonifacio, C. R. Robertson, J. Y. Jung, B. T. King. *J. Org. Chem.* **70**, 8522 (2005).
24. A. Iuliano, P. Piccioli, D. Fabbri. *Org. Lett.* **6**, 3711 (2004).
25. S. K. Collins, A. Grandbois, M. P. Vachon, J. Cote. *Angew. Chem., Int. Ed.* **45**, 2923 (2006).
26. P. M. Donovan, L. T. Scott. *J. Am. Chem. Soc.* **126**, 3108 (2004).
27. H. C. Shen, J. M. Tang, H. K. Chang, C. W. Yang, R. S. Liu. *J. Org. Chem.* **70**, 10113 (2005).
28. M. B. Goldfinger, T. M. Swager. *J. Am. Chem. Soc.* **116**, 7985 (1994).
29. M. B. Goldfinger, K. B. Crawford, T. M. Swager. *J. Am. Chem. Soc.* **119**, 4578 (1997).
30. T. Yao, M. A. Campo, R. C. Larock. *J. Org. Chem.* **70**, 3511 (2005).
31. R. D. Bronene, F. Diederich. *Tetrahedron Lett.* **32**, 5227 (1991).
32. K. A. Muszkat. *Top. Curr. Chem.* **88**, 89 (1981).
33. H. Meier. *Angew. Chem., Int. Ed.* **31**, 1399 (1992).
34. S. X. Xiao, M. Myers, Q. Miao, S. Sanaur, K. L. Pang, M. L. Steigerwald, C. Nuckolls. *Angew. Chem., Int. Ed.* **44**, 7390 (2005).
35. L. T. Scott, P. C. Cheng, M. M. Hashemi, M. S. Bratcher, D. T. Meyer, H. B. Warren. *J. Am. Chem. Soc.* **119**, 10963 (1997).
36. L. T. Scott, M. M. Hashemi, D. T. Meyer, H. B. Warren. *J. Am. Chem. Soc.* **113**, 7082 (1991).
37. L. T. Scott, M. M. Boorum, B. J. McMahon, S. Hagen, J. Mack, J. Blank, H. Wegner, A. de Meijere. *Science* **295**, 1500 (2002).
38. M. M. Boorum, Y. V. Vasil'ev, T. Drewello, L. T. Scott. *Science* **294**, 828 (2001).
39. V. M. Tsefrikas, L. T. Scott. *Chem. Rev.* **106**, 4868 (2006).
40. P. Rempala, J. Kroulik, B. T. King. *J. Am. Chem. Soc*. **126**, 15002 (2004).
41. M. D. Stefano, F. Negri, P. Carbone, K. Müllen. *Chem. Phys.* **314**, 85 (2005).
42. X. Yang, X. Dou, K. Müllen. *Chem. Asia J.* **3**, 759 (2008).
43. X. Dou, W. Pisula, D. Wu, X. Feng, K. Müllen. Unpublished results.
44. X. L. Feng, J. Wu, V. Enkelmann, K. Müllen. *Org. Lett*. **8**, 1145 (2006).
45. X. L. Feng, J. Wu, M. Ai, W. Pisula, L. Zhi, J. P. Rabe, K. Müllen. *Angew. Chem., Int. Ed.* **46**, 3033 (2007).
46. X. L. Feng, W. Pisula, M. Ai, S. Groper, J. P. Rabe, K. Müllen. *Chem. Mater.* **20**, 1191 (2008).
47. X. L. Feng, W. Pisula, M. Takase, V. Enkelmann, K. Müllen. *Chem. Mater.* **20**, 2872 (2008).
48. X. L. Feng, W. Pisula, L. Zhi, M. Takase, K. Müllen. *Angew. Chem., Int. Ed.* **47**, 1703 (2008).
49. X. L. Feng, W. Pisula, T. Kudernac, D. Q. Wu, L. Zhi, S. De Feyter, K. Müllen. *J. Am. Chem. Soc.* **131**, 4439 (2009).
50. C. D. Simpson, J. D. Brand, A. J. Berresheim, L. Przybilla, H. J. Rader, K. Müllen. *Chem.—Eur. J.* **8**, 1424 (2002).
51. F. Dötz, J. D. Brand, S. Ito, L. Gherghel, K. Müllen. *J. Am. Chem. Soc.* **122**, 7707 (2002).
52. Z. Tomovic, M. Watson, K. Müllen. *Angew. Chem., Int. Ed.* **43**, 755 (2004).
53. X. Yang, X. Dou, A. Rouhanipour, L. Zhi, H. J. Räder, K. Müllen. *J. Am. Chem. Soc.* **130**, 4216 (2008).
54. S. E. Stein, R. L. Brown. *J. Am. Chem. Soc.* **109**, 3721 (1987).
55. Z. H. Wang, Z. Tomovic, M. Kastler, R. Pretsch, F. Negri, V. Enkelmann, K. Müllen. *J. Am. Chem. Soc.* **126**, 7794 (2004).
56. M. Kastler, J. Schmidt, W. Pisula, D. Sebastiani, K. Müllen. *J. Am. Chem. Soc.* **128**, 9526 (2006).
57. X. Feng, W. Pisula, K. Müllen. *J. Am. Chem. Soc.* **129**, 14116 (2007).
58. M. Takase, V. Enkelmann, D. Sebastiani, M. Baumgarten, K. Müllen. *Angew. Chem., Int. Ed.* **46**, 5524 (2007).
59. S. Kumar. *Chem. Soc. Rev.* **35**, 83 (2006).
60. S. Sergeyev, W. Pisula, Y. H. Geerts. *Chem. Soc. Rev.* **36**, 1902 (2007).
61. S. Chandrasekhar, B. K. Sadashiva, K. A. Suresh. *Pramana* **9**, 471 (1977).
62. I. Dierking. *Textures of Liquid Crystals*, Wiley-VCH, Weinheim (2003).

63. V. S. K. Balagurusamy, S. K. Prasad, S. Chandrasekhar, S. Kumar, M. Manickam, C. V. Yelamaggad. *Pramana* **53**, 3 (1999).
64. N. Boden, R. J. Bushby, A. N. Cammidge, J. Clements, R. Luo. *Mol. Cryst. Liq. Cryst.* **261**, 251 (1995).
65. Y. Yamamoto, T. Fukushima, W. Jin, A. Kosaka, T. Hara, T. Nakamura, A. Saeki, S. Seki, S. Tagawa, T. Aida. *Adv. Mater.* **18**, 1297 (2006).
66. A. M. van de Craats, J. M. Warman, A. Fechtenkötter, J. D. Brand, M. A. Harbison, K. Müllen. *Adv. Mater*. **11**, 1469 (1999).
67. N. Boden, B. Movaghar. In *Handbook of Liquid Crystals*, Vol. 2B, D. Demus, J. Goodby, G. W. Gray, H. W. Spiess, V. Vill (Eds.), Chap. IX, Wiley-VCH, Weinheim (1998).
68. M. O'Neill, S. M. Kelly. *Adv. Mater.* **15**, 1135 (2003).
69. H. Eichorn. *J. Porphyrins Phthalocyanines* **4**, 88 (2000).
70. B. A. Gregg, M. A. Fox, A. J. Bard. *J. Am. Chem. Soc*. **111**, 3024 (1989).
71. N. Bodon, R. J. Bushby, A. N. Cammidge. *J. Chem. Soc., Chem. Commun.* 465 (1994).
72. N. Boden, R. J. Bushby, A. N. Cammidge. *J. Am. Chem. Soc.* **117**, 924 (1995).
73. J. Zhang, J. S. Moore. *J. Am. Chem. Soc.* **116**, 2655 (1994).
74. S. Hoger, V. Enkelmann, K. Bonrad, C. Tschierske. *Angew. Chem., Int. Ed.* **39**, 2268 (2000).
75. U. Rohr, P. Schlichting, A. Böhm, M. Gross, K. Meerholz, C. Bräuchle, K. Müllen. *Angew. Chem., Int. Ed.* **37**, 1434 (1998).
76. C. Goltner, D. Pressner, K. Müllen, H. W. Spiess. *Angew. Chem., Int. Ed.* **32**, 1660 (1993).
77. B. A. Gregg, R. A. Cormier. *J. Am. Chem. Soc.* **123**, 7959 (2001).
78. N. Boden, R. C. Borner, R. J. Bushby, J. Clements. *J. Am. Chem. Soc.* **116**, 10807 (1994).
79. W. Pisula, Z. Tomovic, C. Simpson, K. Kastler, T. Pakula, K. Müllen. *Chem. Mater.* **17**, 4296 (2005).
80. L. Piot, A. Marchenko, J. Wu, K. Müllen, D. Fichou. *J. Am. Chem. Soc.* **127**, 16245 (2005).
81. F. Jackel, M. D. Watson, K. Müllen, J. P. Rabe. *Phys. Rev. Lett.* **92**, 188303 (2004).
82. M. Ai, S. Groeper, W. Zhuang, X. Dou, X. Feng, K. Müllen, J. P. Rabe. *Appl. Phys. A* **93**, 277 (2008).
83. L. Piot, C. Marie, X. Feng, K. Müllen, D. Fichou. *Adv. Mater.* **20**, 3854 (2008).
84. M. Palma, J. Levin, V. Lemaur, A. Liscio, V. Palermo, J. Cornil, Y. Geerts, M. Lehmann, P. Samori. *Adv. Mater.* **18**, 3313 (2006).
85. J. M. Hoeben, P. Jonkheijm, E. W. Meijer, A. P. H. J. Schenning. *Chem. Rev.* **105**, 1491 (2005).
86. H. N. Tsao, H. J. Rader, W. Pisula, A. Rouhanipour, K. Mullen. *Phys. Status Solidi* **205**, 421 (2008).
87. D. Adam, P. Schuhmacher, J. Simmerer, L. Häussling, K. Siemensmeyer, K. H. Etzbach, H. Ringsdorf, D. Haarer. *Nature* **371**, 141 (1994).
88. W. Pisula, Z. Tomovic, M. D. Watson, K. Müllen, J. Kussmann, C. Ochsenfeld, T. Metzroth, J. Gauss. *J. Phys. Chem. B* **111**, 7481 (2007).
89. X. L. Feng, V. Marcon, W. Pisula, M. R. Hansen, J. Kirkpatrick, D. Andrienko, K. Kremer, K. Müllen. *Nat. Mater.* **8**, 421 (2009).
90. W. Pisula, A. Menon, M. Stepputat, I. Lieberwirth, U. Kolb, A. Tracz, H. Sirringhaus, T. Pakula, K. Müllen. *Adv. Mater.* **17**, 684 (2005).
91. A. M. van de Crass, N. Stutzmann, O. Bunk, M. M. Nielsen, M. D. Watson, K. Müllen, H. D. Chanzy, H. Sirringhaus, R. H. Friend. *Adv. Mat.* **15**, 495 (2003).
92. S. Gunes, H. Neugebauer, N. S. Saricifci. *Chem. Rev.* **107**, 1324 (2007).
93. L. Schmidt-Mende, A. Fechtenkotter, K. Müllen, E. Moons, R. H. Friend, J. D. MacKenzie. *Science* **293**, 1119 (2001).
94. X. Feng, M. Liu, W. Pisula, M. Takase, J. Li, K. Müllen. *Adv. Mater.* **20**, 2684 (2008).
95. T. Christ, B. Glüsen, A. Greiner, A. Kettner, R. Sander, V. Stümpflen, V. Tsukruk, J. H. Wendorff. *Adv. Mater.* **9**, 48 (1997).

96. A. M. van de Craats, J. M. Warman, P. Schlichting, J. Rohr, Y. Geerts, K. Müllen. *Synth. Met.* **102**, 1550 (1999).
97. A. Bacher, C. H. Erdelen, W. Paulus, H. Ringsdorf, H. W. Schmidt, P. Schuhmacher. *Macromolecules* **32**, 4551 (1999).